High sea surface temperatures in tropical warm pools during the Pliocene

Charlotte L. O'Brien[1, 2, 3*], Gavin L. Foster[4], Miguel A. Martínez-Botí[4], Richard Abell[5], James W. B. Rae[6] and Richard D. Pancost[1, 2]

[1]*Organic Geochemistry Unit, School of Chemistry, University of Bristol, Bristol, BS8 1TS, UK*

[2]*Cabot Institute, University of Bristol, Bristol, BS8 1UJ, UK*

[3]*Department of Earth Sciences, University of Oxford, Oxford, OX1 3AN, UK*

[4]*Ocean and Earth Science, National Oceanography Centre Southampton, University of Southampton, Southampton, SO14 3ZH, UK*

[5]*Scottish Marine Institute, Oban, Argyll, PA37 1QA, UK*

[6]*Department of Earth Sciences, Irvine Building, University of St Andrews, St Andrews, KY16 9AL, UK*

*email: charlotte.obrien@earth.ox.ac.uk

The western warm pools of the Atlantic and Pacific Oceans are a critical store of heat and power for the tropical climate system, such that accurately reconstructing past tropical sea surface temperatures is essential for understanding global climate history. Current low latitude Pliocene-to-recent climate reconstructions indicate that sea surface temperatures in the tropical warm pools have remained stable since the early Pliocene, despite 3-4 °C of global cooling. This is commonly thought to imply the operation of some sort of thermostatic regulation. An alternative possibility, that we explore here, is that this apparent stability is the result of the inability of certain geochemical proxy methods to accurately resolve sea surface temperatures in the Pliocene warm pool. We use both inorganic- and organic-proxies to reconstruct sea surface temperatures from the South China Sea, Caribbean and Western Equatorial Pacific. This new multi-proxy reconstruction indicates that in contrast to earlier findings, the western Pacific and western Atlantic warm pools during the Pliocene were ~2 °C warmer than today. Consequently, no thermostat mechanism limited the temperature of the warm pools of the Pliocene equatorial ocean.

The Western Pacific Warm Pool, comprising the warmest surface waters (>28 °C) of the global oceans, is the main source area of heat and water vapour export to high latitudes[1] (Fig. 1). Similarly, the equatorial Atlantic warm pool, although substantially smaller (Fig. 1), represents another important source of moisture and heat to the Northern Hemisphere[2]. Variations in the size and intensity of these warm pool regions, on intra-annual through to geological timescales, influence Walker and Hadley circulations and likely played a major role in the evolution of global climate

since at least the Pliocene, the last time the Earth was significantly warmer than today[3]. Both modelling and proxy-based studies suggest much greater warmth at higher latitudes during the Pliocene[4]. Yet, despite an expansion of the warm pools, current Pliocene to recent sea surface temperature (SST) reconstructions indicate that SSTs in these tropical regions have remained stable for at least the last 5 Myr[5,6] (Fig. 2c), implying the operation of some sort of thermostatic regulation[7,8]. Ocean thermostat hypotheses generally invoke one or a combination of evaporative feedback processes, cloud-SST feedbacks and ocean heat transport mechanisms to restrict maximum tropical ocean SSTs[7,8]; however, recent studies have demonstrated the concept of a strict SST upper limit to be false[9,10]. Although stable tropical SSTs and reduced pole-equator temperature gradients in the Pliocene may imply the existence of an ocean thermostat[6,11], modelling studies and Quaternary palaeo-records[12,13] indicate that temperatures in the warm pool scale with both cooler and warmer global temperatures. We therefore explore an alternative hypothesis here, that Pliocene warm pool SST 'stability' may be the result of inherent proxy-bias[11].

Most Pliocene SST estimates depend on either the alkenone unsaturation temperature proxy ($U^{k'}_{37}$) or Mg/Ca ratios in planktic foraminiferal calcite[6,14]. However, both of these proxy systems have significant limitations when applied to the Pliocene warm pool. An advantage of the $U^{k'}_{37}$-SST proxy is that the values are not directly controlled by seawater chemistry[15], which may vary over time. However, application of the $U^{k'}_{37}$-SST proxy for the Pliocene is restricted, as this proxy is insensitive to temperatures >29 °C[15] and is therefore incapable of resolving SSTs in the warmest ocean regions. Under these conditions, the Mg/Ca-SST proxy is more commonly applied, although this technique also suffers weaknesses, including a sensitivity to

66 salinity, [CO_3^{2-}], dissolution, and diagenesis (see Supplementary Information for
67 relevant references and discussion). Of particular importance on million-year
68 timescales is the fact that accurate conversion of foraminiferal Mg/Ca ratios to SST
69 requires secular changes in seawater composition to be taken into account (e.g. ref.
70 16). The residence times of Mg, ~13 Myr, and Ca, ~1 Myr, in seawater imply that
71 Mg/Ca_{sw} is likely to have varied on timescales >1 Myr. Indeed, both model and proxy
72 data suggest Mg/Ca_{sw} during the Pliocene was broadly lower than today, with
73 estimates ranging from 2.68 to 5.46 mol mol^{-1} compared to the modern value of
74 5.17 mol mol^{-1} (refs 17-21). Correction for changes in Mg/Ca_{sw} has a significant
75 influence on reconstructions of thermal-stasis in the warm pool, yet significant debate
76 exists about the magnitude of this correction, or even if it is required at all (e.g. refs
77 16,22).
78
79 **Revised estimates of tropical warmth**
80 Here we shed new light on Plio-Pleistocene warm pool evolution, by employing a
81 multiple SST-proxy approach at two warm pool sites: South China Sea ODP Site
82 1143 and Caribbean Sea ODP Site 999 (Fig. 1). These sites are well suited for warm
83 pool SST reconstruction, being located within the western Pacific Warm Pool and
84 western Atlantic Warm Pool regions, respectively. Furthermore, these warm pool
85 sites exhibit little intra-annual variability today (<2.7 °C), and have deep mixed layers
86 (>30 m), reducing the likelihood of SST proxy discrepancies due to seasonality or
87 changes in habitat depths. We present a new TEX^{H}_{86}-SST record for Site 1143 and
88 new Mg/Ca-SST data for Sites 1143 and 999 for the Pliocene to recent, and we then
89 compare these with existing $U^{k'}_{37}$- and Mg/Ca-SST records from the same locations[23-
90 26]. The TEX^{H}_{86} (TetraEther index of tetraethers consisting of 86 carbon atoms) proxy

is a relatively new palaeo-SST technique and thus far has only been applied to reconstruct Pliocene SSTs in a few locations (e.g. ref. 27). In comparison with $U^{k'}_{37}$-SST estimates, the TEX^{H}_{86} proxy is not subject to a warm temperature limit until ocean temperatures exceed ~38 °C, nor does this proxy suffer from changes in ocean chemistry or preservation. The TEX^{H}_{86} proxy is not without its own limitations: in particular, TEX^{H}_{86}-derived temperatures can reflect subsurface conditions in some settings[27] and for the Eocene TEX^{H}_{86}-SSTs at high latitudes appear to have a high temperature bias[28]. However, because its limitations are very different from those of the Mg/Ca and $U^{k'}_{37}$ proxies, TEX^{H}_{86} palaeothermometry is a useful independent technique for reconstructing warm Pliocene SSTs.

We find that in the southern South China Sea the $U^{k'}_{37}$ and TEX^{H}_{86} proxies yield similar SSTs throughout the Pleistocene. Moreover, $U^{k'}_{37}$- and TEX^{H}_{86}-SSTs from Holocene samples yield temperatures of ~28 °C[23,29], which agree well with modern mean annual SSTs at Site 1143 (28.4 °C; WOA09)[30]. These observations suggest that both proxies accurately record surface water conditions during the Pleistocene, and likely also on longer timescales, in the southern South China Sea (Fig. 2; Supplementary Figure 3). Furthermore, TEX^{H}_{86} may serve as an accurate SST recorder at temperatures above 29 °C, when the $U^{k'}_{37}$ proxy becomes unresponsive.

For the past ~2 Myr, South China Sea SST-reconstructions from TEX^{H}_{86} and $U^{k'}_{37}$ exhibit similar absolute values, and both show a ~1-2 °C cooling trend (Fig. 2a), clearly arguing against a tropical thermostat at this site. During the Pliocene, ~5.0 to 2.6 Myr, TEX^{H}_{86}-SST estimates indicate even warmer conditions, varying between 27.3 and 30.9 °C. This yields an overall cooling of ~2.2 °C for the Pliocene to recent

(Fig. 2a). These SSTs are slightly warmer than $U^{k'}_{37}$-SST estimates (Fig. 2a), which remain approximately constant at ~28.8 °C. Therefore, the apparent 'stabilisation' of $U^{k'}_{37}$-derived temperature at Site 1143 during the Pliocene appears to be a consequence of its temperature limit (~29 °C), rather than the operation of a thermostat. Thus, the TEX^{H}_{86}-and $U^{k'}_{37}$-SST[23] estimates together confirm that the southern South China Sea warm pool was ~2 °C warmer in the Pliocene relative to today, with cooling occurring from the early-mid Pliocene.

In contrast to TEX^{H}_{86}- and $U^{k'}_{37}$-SST estimates, Pliocene *G. sacculifer* Mg/Ca-SST estimates at Site 1143 are significantly cooler than today, offset by ~2.8 °C relative to TEX^{H}_{86}-SSTs, and remaining stable for the interval ~4.8 to 2.6 Myr, before displaying a warming trend of ~1 °C for the period 2.6 to 1.7 Myr (Fig. 2a). A high-resolution Plio-Pleistocene *G. ruber* Mg/Ca-SST record[31] for the same site also yields cooler (>1 °C) temperatures relative to TEX^{H}_{86} and $U^{k'}_{37}$ for the interval 3.3-2.5 Myr (Fig. 2a). For the past 1.5 Myr, however, *G. sacculifer* Mg/Ca-SST estimates yield similar absolute values to TEX^{H}_{86}- and $U^{k'}_{37}$-SST estimates, as well as displaying a similar subtle cooling trend through this interval (Fig. 2a).

At the tropical Caribbean Sea Site 999, Mg/Ca-SST estimates from surface-dwelling foraminifera *G. ruber*[25,32] and *G. sacculifer* also exhibit good agreement with $U^{k'}_{37}$–SST estimates[25] for the past 2 Myr (Fig. 2b). Similar to Site 1143, *G. sacculifer* Mg/Ca-SSTs record conditions ~1 °C cooler than those indicated by *G. ruber* Mg/Ca-SSTs, reflecting the deeper mixed layer habitat of *G. sacculifer* (Fig. 2b). Prior to 2.6 Myr, however, Site 999 *G. ruber* and *G. sacculifer* Mg/Ca indicate significantly

cooler Pliocene SSTs, by ~1.2 to 3 °C, than those derived from comparable $U^{k'}_{37}$-SST records[25,26] (Fig. 2b).

Temporal trends in Mg/Ca- and organic-SST estimates clearly diverge during the Pliocene at Sites 1143 and 999, although it should be noted that these data do lie within calibration error (Fig. 2). In this instance, however, the determination of absolute temperature estimates is not as important as the temporal trends we reconstruct for the different proxies, which are, in each case, greater than the associated analytical uncertainty.

Causes of sea surface temperature discrepancies

The magnitude and direction of offsets in Pliocene Mg/Ca-SSTs relative to organic-proxy estimates cannot simply be explained by seasonality. These sites are located in warm pool regions with little seasonal variability[33], and today both species (*G. ruber* and *G. sacculifer*) record mean annual SSTs everywhere between 20° N and 20° S (*G. ruber* within ± 1 °C of mean annual SST and *G. sacculifer* the same or slightly cooler than *G. ruber*)[34]. Similarly, the depth habitat of these species is unlikely to vary significantly, since both *G. sacculifer* and *G. ruber* are symbiont bearing; for both to record temperatures lower than $U^{k'}_{37}$ would require migration out of the mixed layer, which is inconsistent with their physiology[35]. We also judge the influence of salinity change, [CO_3^{2-}], partial dissolution and/or diagenesis to be minor (see Supplementary Information for full discussion). Instead, the similarity in the Mg/Ca records from our two widely separated sites and for both species of foraminifera, together with the observed temporal deviation from the organic proxy records, suggests a universal driver. In combination with the documented dependence of

foraminiferal Mg/Ca on Mg/Ca_{sw} (e.g. ref. 36 and references therein) and the likely change of this parameter over the last 5 million years[19], we suggest that the underestimation of Pliocene Mg/Ca-SST estimates in the southern South China Sea and tropical Caribbean Sea relative to organic SST proxy estimates is at least in part a consequence of lower Mg/Ca_{sw} in the Pliocene.

Exploring the effect of seawater Mg/Ca changes on Mg/Ca-SSTs

To investigate the effect of secular changes in Mg/Ca_{sw} on Pliocene Mg/Ca-SST records from warm pool regions, we adjust our Mg/Ca-SST estimates for changes in Mg/Ca_{sw} ($MgCa_{Cor}$; following the approach of ref. 36) using a best fit of data–based estimates[17,18,21,37] (DBF) and also for a variety of different Mg/Ca_{sw} model predictions (FD06[19], HS12[38], SH98[20] and WA89[39]; Fig. 3b, Supplementary Figure 7; for details see Supplementary Information). Adjusting foraminiferal calcite Mg/Ca values for changes in Mg/Ca_{sw} raises Pliocene Mg/Ca-SST estimates at Sites 1143 and 999 by varying degrees, depending on the magnitude of Mg/Ca_{sw} change in the different models/data estimates (Fig. 3b). The FD06[19] correction gives the highest Mg/Ca-SST_{cor} values, while other model estimates (HS12[38], SH98[20] and WA89[39]; Fig. 3b) and the DBF reconstruction (Fig. 3b) are lower and more similar to each other. Nonetheless, accounting for lower Mg/Ca_{sw} clearly reduces the offset between Mg/Ca- and organic-SST estimates in the Pliocene. Even with the most dramatic correction Mg/Ca-SSTs are still somewhat lower (~0.8 °C relative to TEX^{H}_{86}-SSTs at Site 1143 with the Mg/Ca_{sw} of FD06[19]; Fig. 3b), perhaps reflecting other environmental controls, but still display a clear cooling trend similar to TEX^{H}_{86}-SSTs for the past 5 Myr, albeit with a smaller magnitude. An alternative approach to using model predictions of Mg/Ca_{sw} is to assume that all of the discrepancy between

190 TEX^{H}_{86} and Mg/Ca at Site 1143 is due to Mg/Ca_{sw} and generate a record of Mg/Ca_{sw}
191 through 'back–calculating' this parameter from paired foraminiferal Mg/Ca and
192 TEX^{H}_{86} measurements. This record gives slightly larger Mg/Ca_{sw} changes than the
193 FD06[19] model but is largely consistent with the available data constraints
194 (Supplementary Figure 8).
195
196 This treatment of our SST proxy comparisons at Sites 1143 and 999 implies that not
197 only are $U^{k'}_{37}$-SSTs in other warm regions (>28 °C) likely to be biased to too low
198 temperatures, but also that the Mg/Ca-SST proxy also could be underestimating SSTs
199 during the Pliocene at other locations. We discuss the impacts of this Mg/Ca_{sw}
200 correction on other Mg/Ca records in the Supplementary Information, but focus here
201 on ODP Site 806[5], which is located in the heart of the modern Western Pacific warm
202 pool (Fig. 1) and has Pliocene Mg/Ca-SSTs similar to or lower than $U^{k'}_{37}$ estimates
203 (Fig. 2c). The Mg/Ca_{sw} correction increases Pliocene Mg/Ca-SSTs into consistency
204 with the $U^{k'}_{37}$-SST proxy (i.e. >29 °C) regardless of whether our back-calculated
205 Mg/Ca_{sw} is used or the modelled values of FD06[19]. Furthermore, when corrected for
206 Mg/Ca_{sw} changes, Site 806 SSTs are ~0.7-1.8 °C warmer than the TEX^{H}_{86} proxy for
207 the southern South China Sea (Fig. 3c). The existence of this temperature gradient is
208 also evident from the raw *G. sacculifer* Mg/Ca data for the two sites (Mg/Ca of
209 ~3.2 mmol mol^{-1} versus ~3.5 mmol mol^{-1}; equivalent to ~1 °C difference;
210 Supplementary Figures 12 and 13), supporting the veracity of the Mg/Ca_{sw} correction.
211 It is important to note that, whilst we have demonstrated here that secular changes in
212 Mg/Ca_{sw} has likely had dramatic implications for the Mg/Ca-SST proxy in the
213 Pliocene, future work is required to better empirically and directly determine past
214 variations in Mg/Ca_{sw}. Moreover, it does not preclude the influence of other factors

on the Mg/Ca records from Sites 999, 1143 or elsewhere, and additional studies on the partitioning of Mg into foraminiferal calcite as a function of Mg/Ca_{sw}, and further quantification of the secondary effects on Mg/Ca in foraminifer shells (e.g. salinity, diagenesis, $[CO_3^{2-}]$) are required.

Climate forcing of tropical temperatures

The potential operation of a tropical thermostat for the warmest regions of the ocean can be explored by examining the response of the warm pool temperature to climate forcing over the last 5 Myr (following the approach of ref. 13). Over the Pleistocene glacial cycles the temperature evolution of the Pacific Warm Pool is largely a function of climate forcing by CO_2 and changes in global albedo due to the waxing and waning of the continental ice sheets[13,40]. Given the Warm Pool SST response to climate forcing (from ice albedo and CO_2) over Pleistocene glacial cycles, a Pliocene CO_2 range of 350 to 450 ppm[25] and sea-level +10 to +30 m higher than today[41], SSTs in the Pliocene at Site 1143 would be expected to be +1-2 °C compared to the modern, and at Site 806 to be +1.5-2.5 °C (Supplementary Figure 14). Our new SST estimates suggest a ~2-3 °C warming at both sites such that Pliocene temperatures are similar to but slightly warmer than expected. This provides further evidence that there is no 'thermostatic' control limiting SSTs in the warmest ocean regions, at least for SSTs up to 32-34 °C.

These new warm pool Pliocene SST reconstructions support the view[36] that pre-Pleistocene Mg/Ca based SST estimates are compromised, possibly by changes in the Mg/Ca ratio of seawater, and indicate that the role of ocean warm pool regions in generating Pliocene warmth has previously[5,6] been underestimated. This recognition

also resolves the discrepancy between previous SST reconstructions[6,42] and the recent Pliocene Model Intercomparison Project results, which predict 2-3 °C warmer warm pool temperatures in the Pliocene than existing data. Moreover, a ~2-3 °C warmer warm pool in the Pliocene implies no mechanism will operate to limit the degree of warmth of the equatorial ocean in coming centuries as the Earth approaches Pliocene-like conditions.

METHODS

Sampling strategy. Sediments from Ocean Drilling Program (ODP) Site 1143 (9°22′N, 113°17′E, water depth 2772 m) were divided such that ca. 10 g of each sample were used for organic biomarker analyses and the rest of the material was used for *Globigerinoides sacculifer* (*G. sacculifer*) foraminiferal calcite analyses. For ODP Site 999 (12°45'N, 78°44'W, 2828 m water depth), *Globigerinoides ruber* (*G. ruber*) trace element analyses were performed on the same sample set as those analysed for alkenones by an earlier study[26] and *G. sacculifer* trace element analyses were carried out on the same sample set as those analysed for alkenones (and in some cases also *G. ruber*) by Seki et al. (2010)[25].

GDGT biomarker analysis. Relative glycerol dibiphytanyl glycerol tetraether (GDGT) biomarker abundances were used to derive TEX_{86} sea surface temperatures (SSTs). Sediments were freeze-dried and manually ground prior to extraction. Total lipid extracts were obtained via 24 h Soxhlet extraction using dichloromethane:methanol (2:1, *v/v*). Total lipid extracts were then separated into apolar (which were archived) and polar fractions using alumina column chromatography. Polar fractions were dissolved in hexane:propanol (99:1, *v/v*),

265 filtered through 0.45 μm PTFE filters, and then analysed for GDGT compounds using
266 High Performance Liquid Chromatography/Atmospheric Pressure Chemical
267 Ionisation-Mass Spectrometry (HPLC/APCI-MS). Filtered polar fractions were
268 analysed at the University of Bristol using a Thermo Scientific TSQ Quantum Access
269 equipped with Accela Autosampler, Accela Pump and Xcalibur software fitted with
270 an Alltech Prevail Cyano column (150 mm x 2.1 mm; 3 μm stationary phase
271 thickness). The injection volume was 20 μl in partial loop-no waste injection setting.
272 GDGTs were eluted isocratically with 99 % A and 1 % B *v*/*v* for the first 7 min, and
273 then a linear gradient to 1.6 % *v*/*v* B in 43 min, where A = hexane and B = *iso*-
274 propanol under a flow rate of 0.2 ml min^{-1}. Detection was achieved using atmospheric
275 pressure positive ion chemical ionisation-mass spectrometry (APCI-MS) analysis of
276 the eluent. Specific conditions were: corona discharge current 4 μA, vaporiser
277 temperature 355 °C, capillary temperature 280 °C and sheath gas 0.15 L min^{-1}. Ion
278 detection was performed in selective ion monitoring (SIM) mode with selected *m/z*
279 values relating to the $[M+H]^+$ (protonated molecular ion) of the isoprenoidal and
280 branched GDGT analytes[43]. The reproducibility of the TEX^H_{86} values was determined
281 to be ± 0.02 (from 37 duplicate analyses, n=116), which is equivalent to ±0.62 °C[44].
282
283 **Foraminiferal Calcite Trace Element Analysis.** Mg/Ca ratios in foraminiferal
284 calcite were used to derive Mg/Ca SSTs. Site 1143 and Site 999 *G. sacculifer*
285 (without sac) samples were prepared and analysed at the University of Bristol. Site
286 999 *G. ruber* (white) samples were prepared and analysed at the University of
287 Southampton. In all cases, aliquots of the sediment assigned for foraminiferal trace
288 element analyses were washed over a 63 μm sieve and dried. *G. sacculifer* (~10-20
289 individuals) and *G. ruber* (120-180 individuals, of which a 7 % aliquot was assigned

for trace element analysis in this study) tests were picked from the 300-355 μm size fraction, gently crushed between two glass slides and transferred to clean vials. All planktic foraminifer samples were cleaned using established oxidative cleaning methods[45], no reductive step was carried out as this is known to dissolve foraminiferal calcite[46]. After cleaning, all samples were dissolved in ~0.15 M HNO_3, centrifuged and transferred to a clean plastic centrifuge tube. *G. sacculifer* trace elements were measured using a Thermo Scientific Element 2 single collector Inductively Coupled Plasma-Mass Spectrometer (ICP-MS) at the University of Bristol, following methods outlined in Foster (2008)[47]. An aliquot was taken and measured for [Ca] in order to matrix-match samples and bracketing standards, and then the remaining solution was diluted to a known Ca concentration, typically 4 mmol l^{-1}, and analysed for trace element composition. Long-term analytical reproducibility for Mg/Ca is ±1.8 % (2 s.d.) based on replicate analysis of consistency standards matched in concentration to dissolved foraminifera solutions. *G. ruber* trace elements were measured using a Thermo Scientific Element 2 single collector ICP-MS at the University of Southampton, following the same approach as outlined for *G. sacculifer*[8]. Final analyses were typically run at 2 mmol l^{-1} Ca. Over the period 2012-2013, analytical reproducibility for Mg/Ca was ±2.7 % (2 s.d.).

ADDITIONAL INFORMATION

Correspondence and requests for materials should be addressed to C.L.O.B.

ACKNOWLEDGEMENTS

This work was supported by a NERC studentship awarded to C.L.O.B. and a NERC standard grant NE/H006273/1 awarded to R.D.P (Principal Investigator) and G.L.F.

(Co-Investigator). R.D.P. also acknowledges the Royal Society Wolfson Research Merit Award. We would like to thank Kirsty Edgar for helpful discussions on diagenesis of foraminifera.

AUTHOR CONTRIBUTIONS

C.L.O.B. collected all the data (except where otherwise noted), interpreted results, and prepared the manuscript and figures. G.L.F. and R.D.P. supervised the project, and aided in interpretation, figure making and editing the manuscript. M.A.M.-B. generated the *G. ruber* Mg/Ca data for Site 999. R.A. and G.L.F. generated the *G. sacculifer* Mg/Ca data for Site 999. J.W.B.R. aided in the collection of *G. sacculifer* Mg/Ca data for Site 1143, figure making and editing the manuscript.

COMPETING FINANCIAL INTERESTS

The authors declare no competing financial interests.

REFERENCES

1 Pierrehumbert, R. Climate change and the tropical Pacific: The sleeping dragon wakes. *Proc. Nat. Acad. Sci.* **97**, 1355-1358 (2000).

2 Wang, C. & Enfield, D. B. The tropical Western Hemisphere warm pool. *Geophys. Res. Lett.* **28**, 1635-1638 (2001).

3 Herbert, T. D., Peterson, L. C., Lawrence, K. T. & Liu, Z. Tropical ocean temperatures over the past 3.5 million years. *Science* **328**, 1530-1534 (2010).

4 Brierley, C. M. *et al.* Greatly expanded tropical warm pool and weakened Hadley circulation in the early Pliocene. *Science* **323**, 1714-1718 (2009).

5 Wara, M. W., Ravelo, A. C. & Delaney, M. L. Permanent El Niño-like conditions during the Pliocene warm period. *Science* **309**, 758-761 (2005).

6 Fedorov, A. *et al.* Patterns and mechanisms of early Pliocene warmth. *Nature* **496**, 43-49 (2013).

7 Ramanathan, V. & Collins, W. Thermodynamic regulation of ocean warming by cirrus clouds deduced from observations of the 1987 El Nino. *Nature* **351**, 27-32 (1991).

8 Newell, R. E. Climate and the Ocean: Measurements of changes in sea-surface temperature should permit us to forecast certain climatic changes several months ahead. *Am. Sci.* **67**, 405-416 (1979).

9 Williams, I. N., Pierrehumbert, R. T. & Huber, M. Global warming, convective threshold and false thermostats. *Geophys. Res. Lett.* **36**, L21805 (2009).

10 van Hooidonk, R. & Huber, M. Equivocal evidence for a thermostat and unusually low levels of coral bleaching in the Western Pacific Warm Pool. *Geophys. Res. Lett.* **36** (2009).

11 Medina-Elizalde, M. & Lea, D. W. Late Pliocene equatorial Pacific. *Paleoceanography* **25**, PA2208 (2010).

12 Lea, D. W., Pak, D. K. & Spero, H. J. Climate Impact of Late Quaternary Equatorial Pacific Sea Surface Temperature Variations. *Science* **289**, 1719-1724 (2000).

13 Rohling, E., Medina-Elizalde, M., Shepherd, J., Siddall, M. & Stanford, J. Sea surface and high-latitude temperature sensitivity to radiative forcing of climate over several glacial cycles. *J. Climate* **25**, 1635-1656 (2012).

14 Dowsett, H. J. *et al.* Assessing confidence in Pliocene sea surface temperatures to evaluate predictive models. *Nature Clim. Change* **2**, 365-371 (2012).

15 Müller, P. J., Kirst, G., Ruhland, G., Von Storch, I. & Rosell-Melé, A. Calibration of the alkenone paleotemperature index UK'37 based on core-tops from the eastern South Atlantic and the global ocean (60 N-60 S). *Geochim. Cosmochim. Acta* **62**, 1757-1772 (1998).

16 Medina-Elizalde, M., Lea, D. W. & Fantle, M. S. Implications of seawater Mg/Ca variability for Plio-Pleistocene tropical climate reconstruction. *Earth Planet. Sci. Lett.* **269**, 585-595 (2008).

17 Coggon, R. M., Teagle, D. A. H., Smith-Duque, C. E., Alt, J. C. & Cooper, M. J. Reconstructing past seawater Mg/Ca and Sr/Ca from mid-ocean ridge flank calcium carbonate veins. *Science* **327**, 1114-1117 (2010).

18 Lowenstein, T. K., Timofeeff, M. N., Brennan, S. T., Hardie, L. A. & Demicco, R. V. Oscillations in Phanerozoic seawater chemistry: Evidence from fluid inclusions. *Science* **294**, 1086-1088 (2001).

19 Fantle, M. S. & DePaolo, D. J. Sr isotopes and pore fluid chemistry in carbonate sediment of the Ontong Java Plateau: Calcite recrystallization rates and evidence for a rapid rise in seawater Mg over the last 10 million years. *Geochim. Cosmochim. Acta* **70**, 3883-3904 (2006).

20 Stanley, S. M. & Hardie, L. A. Secular oscillations in the carbonate mineralogy of reef-building and sediment-producing organisms driven by tectonically forced shifts in seawater chemistry. *Palaeogeogr., Palaeoclimatol., Palaeoecol.* **144**, 3-19 (1998).

21 Rausch, S., Böhm, F., Bach, W., Klügel, A. & Eisenhauer, A. Calcium carbonate veins in ocean crust record a threefold increase of seawater Mg/Ca in the past 30 million years. *Earth Planet. Sci. Lett.* **362**, 215-224 (2013).

22 Dekens, P. S., Ravelo, A. C., McCarthy, M. D. & Edwards, C. A. A 5 million year comparison of Mg/Ca and alkenone paleothermometers. *Geochem. Geophys. Geosyst.* **9**, Q10001 (2008).

23 Li, L. *et al.* A 4-Ma record of thermal evolution in the tropical western Pacific and its implications on climate change. *Earth Planet. Sci. Lett.* **309**, 10-20 (2011).

24 Groeneveld, J. *Effect of the Pliocene closure of the Panamanian Gateway on Caribbean and east Pacific sea surface temperatures and salinities by applying combined Mg/Ca and δ18O measurements (5.6-2.2 Ma)* PhD thesis, University of Kiel, (2005).

25 Seki, O. *et al.* Alkenone and boron-based Pliocene pCO2 records. *Earth Planet. Sci. Lett.* **292**, 201-211 (2010).

26 Badger, M. P., Schmidt, D. N., Mackensen, A. & Pancost, R. D. High-resolution alkenone palaeobarometry indicates relatively stable pCO2 during the Pliocene (3.3–2.8 Ma). *Phil. Trans. R. Soc. A* **371** (2013).

27 Seki, O. *et al.* Paleoceanographic changes in the Eastern Equatorial Pacific over the last 10 Myr. *Paleoceanography* **27**, PA3224 (2012).

28 Hollis, C. J. *et al.* Early Paleogene temperature history of the Southwest Pacific Ocean: Reconciling proxies and models. *Earth Planet. Sci. Lett.* **349**, 53-66 (2012).

29 Wei, Y. *et al.* Spatial variations in archaeal lipids of surface water and core-top sediments in the South China Sea and their implications for paleoclimate studies. *Appl. Environ. Microbiol.* **77**, 7479-7489 (2011).

30 Locarnini, R. A. *et al.* in *NOAA Atlas NESDIS 68* Vol. 1 (ed S. Levitus) 184 (U.S. Government Printing Office, 2010).

31 Tian, J. *et al.* Late Pliocene monsoon linkage in the tropical South China Sea. *Earth Planet. Sci. Lett.* **252**, 72-81 (2006).

32 Schmidt, M. W., Vautravers, M. J. & Spero, H. J. Western Caribbean sea surface temperatures during the late Quaternary. *Geochem. Geophys. Geosyst.* **7**, Q02P10 (2006).

33 Wunsch, C. A perpetually running ENSO in the Pliocene? *J. Climate* **22**, 3506-3510 (2009).

34 Fraile, I., Mulitza, S. & Schulz, M. Modeling planktonic foraminiferal seasonality: Implications for sea-surface temperature reconstructions. *Mar. Micropaleontol.* **72**, 1-9 (2009).

35 Hemleben, C., Spindler, M. & Erson, O. *Modern planktonic foraminifera*. (Springer, 1989).

36 Evans, D. & Müller, W. Deep time foraminifera Mg/Ca paleothermometry: Nonlinear correction for secular change in seawater Mg/Ca. *Paleoceanography* **27**, PA4205 (2012).

37 Horita, J., Zimmermann, H. & Holland, H. D. Chemical evolution of seawater during the Phanerozoic: implications from the record of marine evaporites. *Geochim. Cosmochim. Acta* **66**, 3733-3756 (2002).

433 38 Higgins, J. & Schrag, D. Records of Neogene seawater chemistry and
434 diagenesis in deep-sea carbonate sediments and pore fluids. *Earth Planet. Sci.*
435 *Lett.* **357**, 386-396 (2012).
436 39 Wilkinson, B. H. & Algeo, T. J. Sedimentary carbonate record of calcium-
437 magnesium cycling. *Am. J. Sci.* **289**, 1158-1194 (1989).
438 40 Köhler, P. *et al.* What caused Earth's temperature variations during the last
439 800,000 years? Data-based evidence on radiative forcing and constraints on
440 climate sensitivity. *Quat. Sci. Rev.* **29**, 129-145 (2010).
441 41 Rohling, E. J. *et al.* Sea-level and deep-sea-temperature variability over the
442 past 5.3 million years. *Nature* **508**, 477-482 (2014).
443 42 Dowsett, H. J. *et al.* Sea Surface Temperature of the mid-Piacenzian Ocean: A
444 Data-Model Comparison. *Sci. Rep.* **3** (2013).
445 43 Schouten, S., Hopmans, E. C., Schefuß, E. & Sinninghe Damsté, J. S.
446 Distributional variations in marine crenarchaeotal membrane lipids: a new tool
447 for reconstructing ancient sea water temperatures? *Earth Planet. Sci. Lett.* **204**,
448 265-274 (2002).
449 44 Kim, J. H. *et al.* New indices and calibrations derived from the distribution of
450 crenarchaeal isoprenoid tetraether lipids: Implications for past sea surface
451 temperature reconstructions. *Geochim. Cosmochim. Acta* **74**, 4639-4654
452 (2010).
453 45 Barker, S., Greaves, M. & Elderfield, H. A study of cleaning procedures used
454 for foraminiferal Mg/Ca paleothermometry. *Geochem. Geophys. Geosyst.* **4**,
455 8407 (2003).

46 Yu, J., Elderfield, H., Greaves, M. & Day, J. Preferential dissolution of benthic foraminiferal calcite during laboratory reductive cleaning. *Geochem. Geophys. Geosyst.* **8** (2007).

47 Foster, G. L. Seawater pH, pCO2 and [CO2−3] variations in the Caribbean Sea over the last 130 kyr: A boron isotope and B/Ca study of planktic foraminifera. *Earth Planet. Sci. Lett.* **271**, 254-266 (2008).

48 Schlitzer, R. Interactive analysis and visualization of geoscience data with Ocean Data View. *Comput. Geosci.* **28(10)**, 1211-1218 (2002).

49 Pagani, M., Liu, Z., LaRiviere, J. & Ravelo, A. C. High Earth-system climate sensitivity determined from Pliocene carbon dioxide concentrations. *Nature Geosci.* **3**, 27-30 (2009).

50 Lisiecki, L. E. & Raymo, M. E. A Pliocene-Pleistocene stack of 57 globally distributed benthic δ18O records. *Paleoceanography* **20**, PA1003 (2005).

FIGURE CAPTIONS

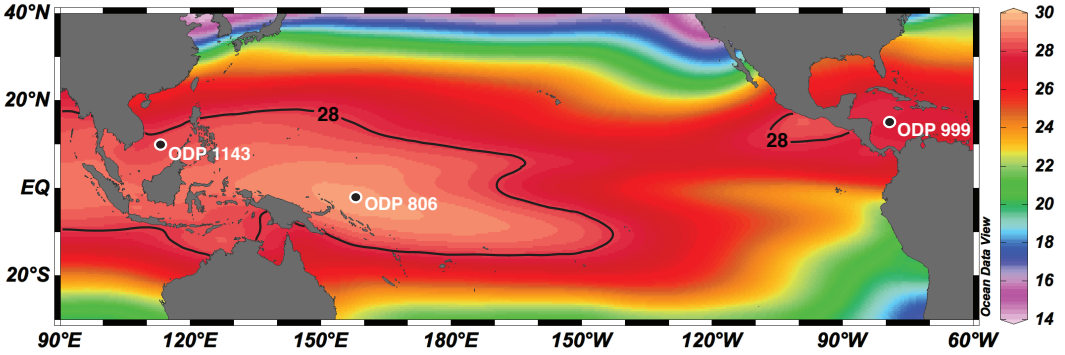

Figure 1: Map of mean annual ocean surface temperatures and locations of the sediment cores discussed in this paper[30,48]. New palaeoceanographic proxy data were generated for ODP Site 1143 (9°22′N, 113°17′E, water depth 2772 m) and ODP Site 999 (12°45'N, 78°44'W, 2828 m water depth). ODP: Ocean Drilling

476 Program. Black line indicates the 28 °C isotherm defining the ocean warm pool

477 regions.

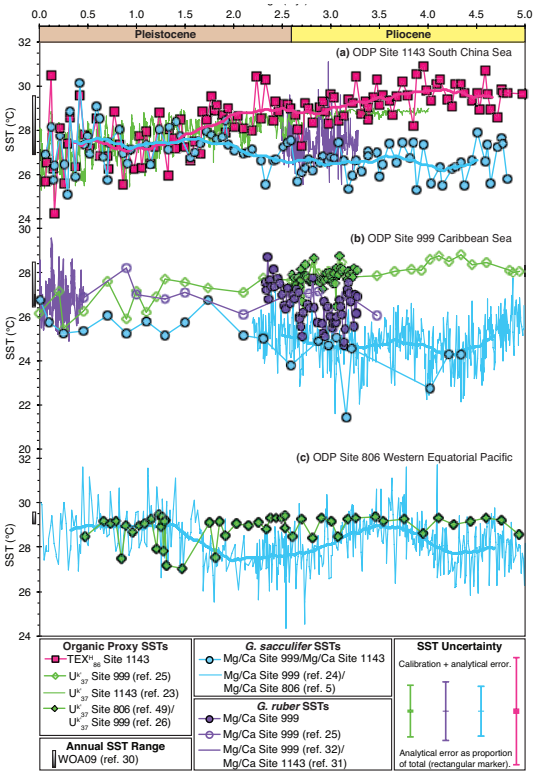

478

479 **Figure 2: Pliocene to recent warm pool SST estimates.** (a) Site 1143 TEX^{H}_{86}-SSTs,

480 *G. sacculifer* Mg/Ca-SSTs, *G. ruber* Mg/Ca-SSTs (ref. 31) and $U^{k'}_{37}$-SSTs (ref. 23).

481 (b) Site 999 *G. ruber* Mg/Ca-SSTs (this study and refs 25,32), *G. sacculifer* SSTs

482 (this study and ref. 24) and $U^{k'}_{37}$-SSTs (refs 25,26). (c) ODP Site 806 *G. sacculifer*

483 Mg/Ca-SSTs (ref. 5) and $U^{k'}_{37}$-SSTs (ref. 49). Thick lines, where included, indicate

484 600 kyr running average smoothing. SST proxy error bars (to scale) include both

485 analytical error ($\sigma_{Analytical}$; $\sigma_{Analytical} = \sigma_{Analytical}^2/(\sigma_{Analytical}^2 + \sigma_{Calibration}^2)$ and calibration

486 error ($\sigma_{Calibration}$; $\sigma_{Calibration} = \sigma_{Calibration}^2/(\sigma_{Analytical}^2 + \sigma_{Calibration}^2)$.

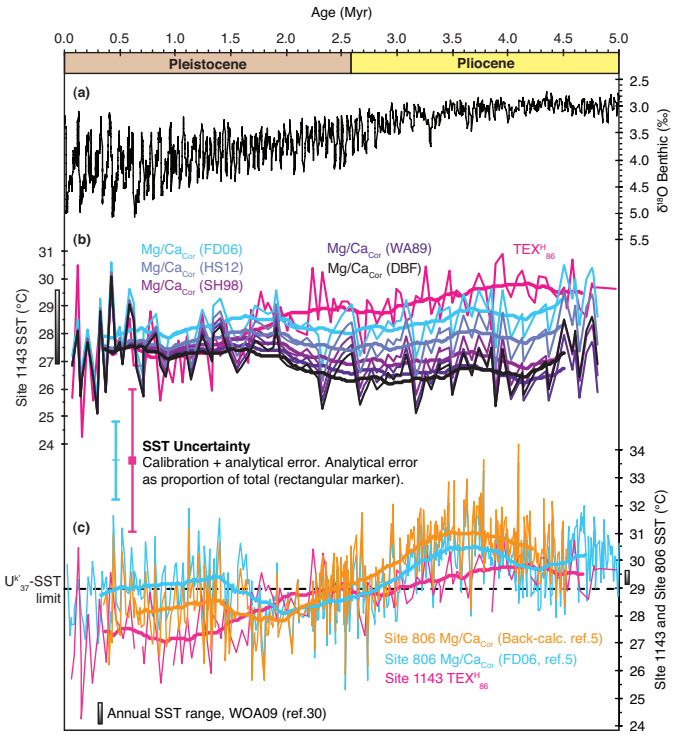

487

488 **Figure 3: Plio-Pleistocene warm pool evolution.** (a) Benthic oxygen isotope stack

489 (ref. 50). (b) Site 1143 TEX^{H}_{86}-SSTs and Mg/Ca-SSTs corrected for variable

490 Mg/Ca_{sw} ($Mg/Ca\text{-}SST_{cor}$) for both data (DBF; refs 17,18,21,37) and Mg/Ca_{sw} model

491 estimates; FD06 (ref. 19), HS12 (ref. 38), SH98 (ref. 20) and WA89 (ref. 39). (c) Site

492 1143 TEX^{H}_{86}-SSTs and Site 806 Mg/Ca-SSTs (ref. 5) corrected for variable Mg/Ca_{sw},

493 $Mg/Ca\text{-}SST_{cor}$, using the FD06 (ref. 19) model and our back-calculated Mg/Ca_{sw}

494 curve. Thick lines indicate 600 kyr running average smoothing. SST proxy error bars,

495 analytical ($\sigma_{Analytical} = \sigma_{Analytical}^2/(\sigma_{Analytical}^2 + \sigma_{Calibration}^2)$ and calibration ($\sigma_{Calibration} =$

496 $\sigma_{Calibration}^2/(\sigma_{Analytical}^2 + \sigma_{Calibration}^2)$, are to scale.